

Supercoiling, knotting and replication fork reversal in partially replicated plasmids

L. Olavarrieta, M. L. Martínez-Robles, J. M. Sogo¹, A. Stasiak², P. Hernández, D. B. Krimer and J. B. Schwartzman*

Departamento de Biología Celular y del Desarrollo, Centro de Investigaciones Biológicas (CSIC), Velázquez 144, 28006 Madrid, Spain, ¹Institut für Zellbiologie ETH-Hönggerberg, CH-8093 Zürich, Switzerland and ²Laboratoire d'Analyse Ultrastructurale, Bâtiment de Biologie, Université de Lausanne, CH-1015 Lausanne, Switzerland

Received October 31, 2001; Revised and Accepted November 23, 2001

ABSTRACT

To study the structure of partially replicated plasmids, we cloned the *Escherichia coli* polar replication terminator TerE in its active orientation at different locations in the ColE1 vector pBR18. The resulting plasmids, pBR18-TerE@*StyI* and pBR18-TerE@*EcoRI*, were analyzed by neutral/neutral two-dimensional agarose gel electrophoresis and electron microscopy. Replication forks stop at the Ter–TUS complex, leading to the accumulation of specific replication intermediates with a mass 1.26 times the mass of non-replicating plasmids for pBR18-TerE@*StyI* and 1.57 times for pBR18-TerE@*EcoRI*. The number of knotted bubbles detected after digestion with *ScaI* and the number and electrophoretic mobility of undigested partially replicated topoisomers reflect the changes in plasmid topology that occur in DNA molecules replicated to different extents. Exposure to increasing concentrations of chloroquine or ethidium bromide revealed that partially replicated topoisomers (CCCRIs) do not sustain positive supercoiling as efficiently as their non-replicating counterparts. It was suggested that this occurs because in partially replicated plasmids a positive ΔLk is absorbed by regression of the replication fork. Indeed, we showed by electron microscopy that, at least in the presence of chloroquine, some of the CCCRIs of pBR18-Ter@*StyI* formed Holliday-like junction structures characteristic of reversed forks. However, not all the positive supercoiling was absorbed by fork reversal in the presence of high concentrations of ethidium bromide.

INTRODUCTION

Brewer–Fangman neutral/neutral (N/N) two-dimensional (2D) agarose gel electrophoresis, originally designed to separate branched from linear molecules (1), has been extensively used to map replication origins, termini and fork barriers in prokaryotes as well as in eukaryotic cells (2). In contrast, the capacity of N/N

2D gels to resolve different forms of undigested plasmids has been exploited far less frequently. Martín-Parras and co-workers (3) used these N/N 2D gels to characterize the different forms a bacterial plasmid can adopt. Topoisomers, catenanes and knotted forms corresponding to non-replicating plasmids were readily identified, but no discrete signal was observed that could be assigned to supercoiled replication intermediates (CCCRIs). When pBR322 was allowed to replicate in *Xenopus* cell extracts, labeled with radioisotopes *in vivo* and analyzed in a 2D gel system where the second dimension occurred in the presence of ethidium bromide, a smeary signal, termed 'Niagara Falls', was detected between the positions where monomeric non-replicating covalently closed circles (CCC) and open circles (OC) migrated in the gel (3). It was argued that this 'Niagara Falls' pattern was generated by partially replicated supercoiled molecules. The signal appeared smeary because RIs with different masses and different ΔLk values exhibit different electrophoretic mobilities. This interpretation is in agreement with observations made for SV40 (4,5) and the 2 μ m plasmid of *Saccharomyces cerevisiae* (6,7).

To prove this hypothesis, we constructed two new plasmids in which specific RIs become accumulated with time. In this way we were able to visualize the supercoiled forms of specific RIs. To force the accumulation of specific RIs, we cloned the *Escherichia coli* polar replication terminator TerE (8,9) at two different locations in the ColE1 vector pBR18. These partially replicated RIs were then analyzed by N/N 2D agarose gel electrophoresis undigested and after digestion with a restriction enzyme that cut the plasmids only once, outside the replicated portion. On the other hand, it was recently proposed that in partially replicated plasmids a positive ΔLk is absorbed by regression of the replication fork (10). We wanted to confirm and extend this observation, studying the effects on these two new plasmids of different concentrations of drugs that are known to affect DNA supercoiling.

The results obtained indicate that plasmid topology changes significantly as replication progresses. As a consequence, the electrophoretic mobility of the whole population of CCCRIs becomes highly heterogeneous. This explains why CCCRIs generate a smeary pattern in N/N 2D gels (3). In addition, treatment with different concentrations of chloroquine and ethidium bromide allowed us to confirm that in partially replicated plasmids the induction of positive supercoiling can

*To whom correspondence should be addressed. Tel: +34 91 5644562; Fax: +34 91 564 8749; Email: schvartzman@cib.csic.es

lead to replication fork reversal (10). However, we found that not all positive supercoiling was absorbed by replication fork reversal in the presence of high concentrations of ethidium bromide.

MATERIALS AND METHODS

Bacterial strains and culture medium

The *E. coli* strain used in this study was DH5 α F'. Competent cells were transformed with monomeric forms of the plasmids as described (11). Cells were grown at 37°C in LB medium containing 50 mg/ml ampicillin.

Plasmid constructs

To construct pBR18-TerE@*StyI* two oligos (5'-CCGAGTTA-AAGTAGTTTGTAAGCTAAGCCC and 3'-CAATTCATAC-AACATTGATTCGGGGTTC) containing the 23 bp that constitute the *E. coli* TerE terminator (8,9) with 3' *StyI* and 5' *AvaI* tails were annealed to each other and inserted between the unique *StyI* and *AvaI* sites of pBR18. To construct pBR18-TerE@*EcoRI* two different oligos (5'-AATTCGGCTTAGTT-ACAACATACTTTAAA and 3'-GCCGAATCAATGTTGT-ATGAAATTTTCGA) including the 23 bp that constitute the *E. coli* TerE terminator (8,9) with 5' *EcoRI* and 3' *HindIII* tails were annealed to each other and inserted between the unique *EcoRI* and *HindIII* sites of pBR18.

Isolation of plasmid DNA

Isolation of the plasmid DNA was performed as described previously (3,12,13).

Two-dimensional gel electrophoresis and Southern transfer

The first dimension was in a 0.4% agarose gel in TBE buffer at 1 V/cm and at room temperature for 20–24 h. The lane containing the λ DNA/*HindIII* marker sizes was excised, stained with 0.3 mg/ml ethidium bromide and photographed. During this, the lanes containing the problem DNA sample were kept in the dark. The second dimension was in a 1% agarose gel in TBE containing 0.3 mg/ml ethidium bromide at 90° with respect to the first dimension. The dissolved agarose was poured around the excised lane from the first dimension and electrophoresis was at 5 V/cm in a 4°C cold chamber for 7–10 h. Southern transfer was performed as described previously (3,12,13).

Non-radioactive hybridization

Probes were labeled using a Random Primer Fluorescein Kit (NEN Life Sciences Products). Membranes were pre-hybridized in a 20 ml pre-hybridization solution (2 \times SSPE, 0.5% Blotto, 1% SDS, 10% dextran sulfate and 0.5 mg/ml sonicated and denatured salmon sperm DNA) at 65°C for 4–6 h. Labeled DNA was added and hybridization lasted 12–16 h. Then, membranes were successively washed with 2 \times SSC and 0.1% SDS for 15 min each at room temperature, except for the last wash, which was at 65°C. Detection was performed with an anti-fluorescein-AP conjugate and CDP-Star (NEN), according to the instructions provided by the manufacturer.

Preparation of DNA samples enriched for specific RIs

Specific molecules were isolated following the procedure described elsewhere (14), with minor modifications. Briefly, plasmid DNA isolated from exponentially growing cells was analyzed in a one-dimensional agarose gel run under the conditions used for the second dimension of the regular 2D gel. A conventional 2D gel with the same sample was run in parallel as an internal control. The 2D gel and a portion of the gel containing the lane with the problem sample were excised, transferred to a nylon membrane and hybridized with a labeled probe. Comparison of the patterns in both gels allowed us to determine the distance migrated by the molecules of interest in the one-dimensional gel. According to this estimation, the portion containing these molecules of interest was excised and electroeluted inside a dialysis bag. The DNA was phenol extracted, ethanol precipitated and resuspended in distilled water.

Electron microscopy

The purified DNA was spread for electron microscopy under non-denaturing conditions onto 100 μ g/ml chloroquine or 0.3 μ g/ml ethidium bromide in redistilled water by the BAC method, except that formamide was added to the spreading solution at a concentration of 15% and the final concentration of BAC was increased to 0.01% (15).

RESULTS

In pBR322, transcription of the constitutive tetracycline-resistance gene occurs against the direction of replication fork movement. This affects supercoiling and leads to the formation of a significant number of knotted molecules (16,17). To avoid this type of knotting, we decided to use pBR18 instead of pBR322 as our cloning vector. pBR18 is a derivative of pBR322 in which the sequence between the unique *EcoRI* and *HindIII* sites of pBR322 has been replaced with the polycloning fragment of pUC18 (13). In doing so, the promoter for the tetracycline resistance gene was lost.

The first plasmid we constructed was pBR18-TerE@*StyI*. The 23 bp that constitute the *E. coli* polar replication terminator TerE (8,9) were inserted between the unique *StyI* and *AvaI* sites of pBR18. We decided to use TerE instead of any of the other *E. coli* terminators because TerE binds TUS with rather weak affinity (18). As depicted in Figure 1A, pBR18-TerE@*StyI* contains a ColE1 replication origin, the TerE replication terminator in its active orientation with respect to the unidirectional ColE1 origin and the copy number control gene *rep*, and confers resistance only to ampicillin. We anticipated that in most plasmids replication forks would stop at the TerE–TUS complex, leading to the accumulation of specific RIs containing an internal bubble and with a total mass 1.26 times the mass of non-replicating plasmids (Fig. 1B).

To confirm this prediction *E. coli* DH5 α F' cells were transformed with pBR18-TerE@*StyI* and the corresponding RIs were analyzed by N/N 2D agarose gel electrophoresis after digestion with *ScaI*. This restriction enzyme cuts pBR18-TerE@*StyI* only once at position 3842 (see Fig. 1A). We used the computer program developed by Viguera and co-workers (19) to predict the shape of the RIs and the 2D gel pattern expected. An autoradiogram of the corresponding gel is shown in Figure 2A, with a diagrammatic interpretation in Figure 2B.

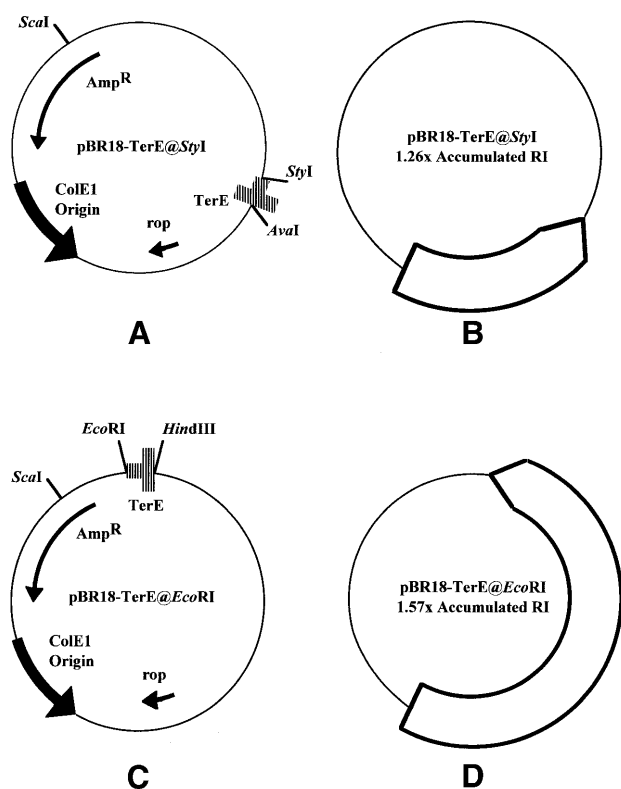


Figure 1. Maps of the plasmids used in this study. (A) Map of pBR18-TerE@StyI showing the relative position of its most relevant features: the ColE1 unidirectional origin, the *E. coli* terminator TerE, the ampicillin resistance and *rop* genes and the recognition sites for a number of restriction endonucleases that cut the plasmid only once. (B) TerE binds the terminator protein TUS and the Ter-TUS complex acts as a polar replication fork barrier. Therefore, blockage of the replication fork at TerE would lead to the accumulation of a specific RI containing an internal bubble with a total mass 1.26 times the mass of non-replicating plasmids. (C) Map of pBR18-TerE@EcoRI showing the position of its most relevant features. (D) In this plasmid, blockage of the replication fork at TerE would lead to the accumulation of a specific RI containing an internal bubble and with a total mass 1.57 times the mass of non-replicating plasmids.

Two signals with comparable intensities were conspicuous. One of them migrated on the arc of linears with a mass equivalent to 4.3 kb. This signal corresponded to linearized unreplicated forms. The other prominent spot migrated on the bubble arc (not visible in this autoradiogram). It corresponded to a partially replicated RI containing an internal bubble that spanned from the ColE1 origin to the TerE sequence. A series of minor spots showing decreasing intensities (like 'beads on a string') were observed to the right of the unknotted bubble and another spot was visible above and to the right. This latter spot migrated similarly to the 1.0 \times linear form in the first dimension but was significantly retarded in the second dimension. It corresponded to nicked OC forms of the monomer. The series of minor spots ('beads on a string') behaved as already reported for partially replicated RIs containing an internal knotted bubble (12,13,20,21).

We wanted to know whether the observations made for pBR18-TerE@StyI also applied to other plasmids having TerE cloned at a different location. To answer this question we

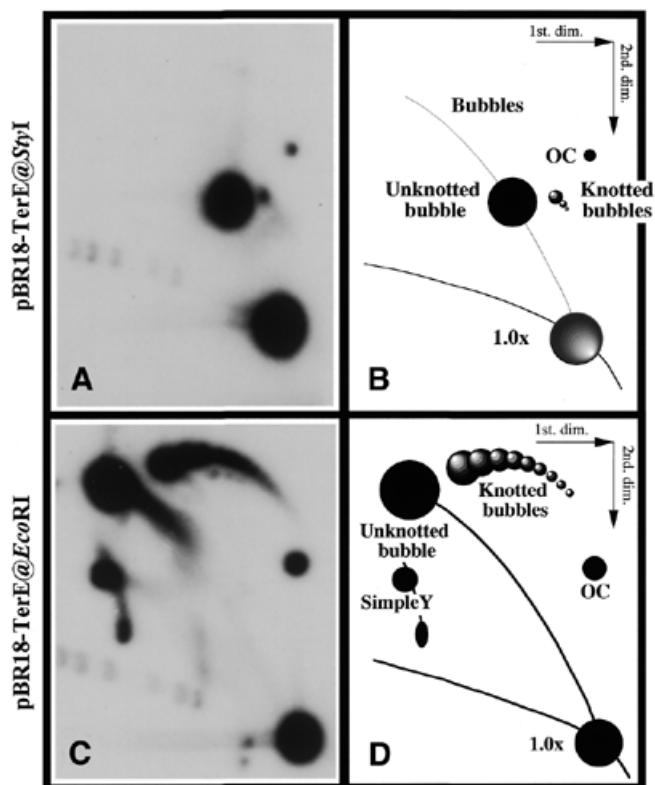


Figure 2. Autoradiograms of 2D gels corresponding to pBR18-TerE@StyI (A) and pBR18-TerE@EcoRI (C) after digestion with *ScaI* and their corresponding diagrammatic interpretations (B and D). Note that the number and complexity of knotted bubbles was significantly higher in pBR18-TerE@EcoRI.

constructed another plasmid, pBR18-TerE@EcoRI. This new plasmid was identical to pBR18-TerE@StyI except that it had the 23 bp that constitute TerE between the unique *EcoRI* and *HindIII* sites of pBR18 (Fig. 1C). Once again, replication forks would stop at the TerE-TUS complex, but in this case fork arrest would lead to the accumulation of specific RIs containing an internal bubble and with a total mass 1.57 times the mass of non-replicating plasmids (Fig. 1D).

Escherichia coli DH5 α F' cells were transformed with pBR18-TerE@EcoRI and the corresponding RIs were analyzed by N/N 2D agarose gel electrophoresis after digestion with *ScaI*. As with the former plasmid, we used the computer program developed by Viguera and co-workers (19) to predict the shapes of the RIs and the 2D gel patterns expected. In this new plasmid TerE is located 2481 bp downstream of the origin (Fig. 1C). Therefore, the accumulated RIs with an internal bubble would have a relative mass 1.57 times the mass of unreplicated linear molecules (Fig. 1D). An autoradiogram of the corresponding gel is shown in Figure 2C, with a diagrammatic interpretation in Figure 2D. The unreplicated linear form (1.0 \times) was clearly distinguished on the arc of linears at the bottom of the autoradiogram. The partially replicated RI (unknotted bubble) was also evident on top of the bubble arc. The number and intensity of the spots corresponding to knotted bubbles ('beads on a string' signal) increased significantly

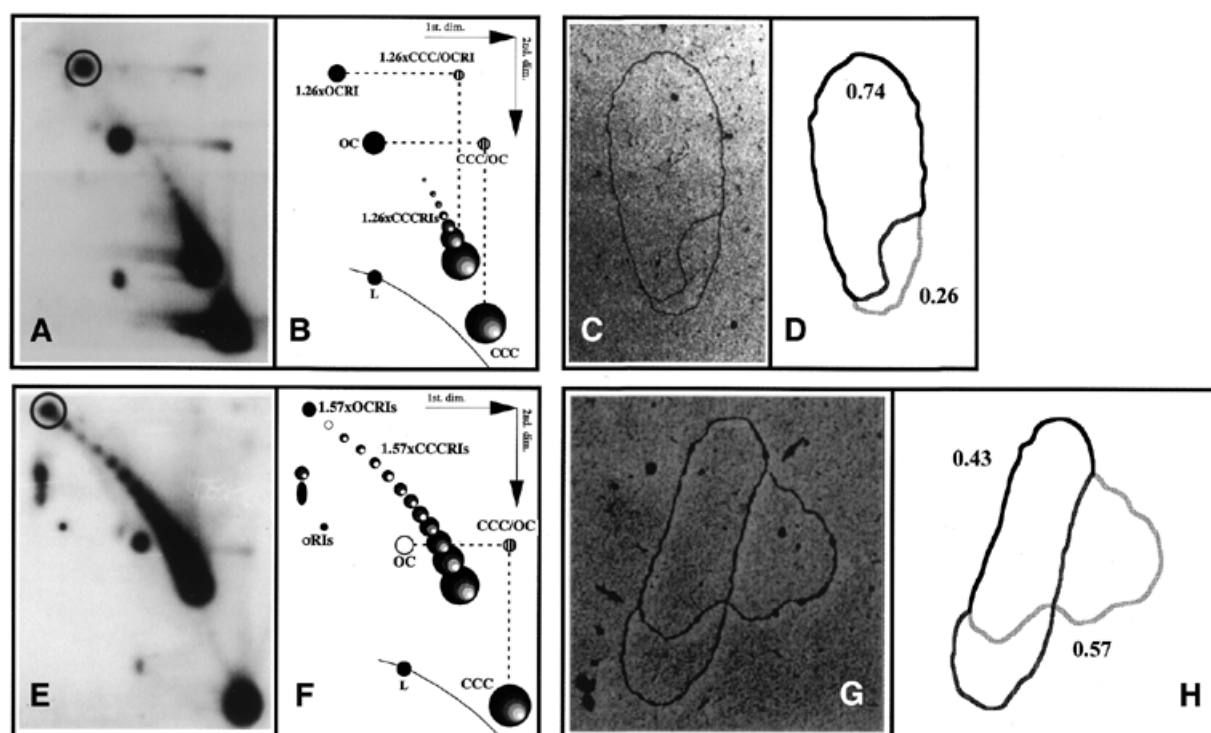


Figure 3. 2D gels and electron microscopy confirmed that *in vivo* partially replicated forms of pBR18-TerE@StyI and pBR18-TerE@EcoRI accumulated with the predicted masses. (A) 2D gel of intact forms of pBR18-TerE@StyI. (B) Diagrammatic interpretation of the different signals observed in the autoradiogram shown in (A). (C) Electron microscopy of a selected molecule that was eluted from the signal circled in (A). (D) Diagrammatic interpretation of the electron micrograph shown in (C). The black line represents unreplicated DNA while the stippled lines represent replicated arms. Numbers denote the percentage contour length of unreplicated and replicated arms, respectively. (E) 2D gel of intact forms of pBR18-TerE@EcoRI. (F) Diagrammatic interpretation of the different signals observed in the autoradiogram shown in (E). (G) Electron micrograph of a selected molecule that was eluted from the signal circled in (E). (H) Diagrammatic interpretation of the electron micrograph shown in (G). As in the previous case, the black line represents unreplicated DNA while the stippled lines represent replicated arms. Numbers denote the percentage contour length of unreplicated and replicated arms. CCC, covalently closed circle; OC, open circle; RIs, replication intermediates; oRIs, broken replication intermediates; L, linears.

when compared to pBR18-TerE@StyI (see Fig. 2A). In addition, the OC form and a double-Y pattern were also apparent.

To further confirm the nature of these plasmids, undigested pBR18-TerE@StyI DNA was analyzed by a modified Brewer-Fangman N/N 2D agarose gel electrophoresis (6) in which ethidium bromide was omitted for the second dimension. An autoradiogram of the corresponding gel is shown in Figure 3A with a diagrammatic interpretation in Figure 3B. It was previously shown that intact supercoiled molecules are easily nicked during DNA isolation (2,6,11,22,23). Nicking can also occur as the first dimension proceeds, between the first and the second dimensions and throughout the second dimension electrophoresis. As a consequence, a horizontal trailing signal arises if nicking occurred in the first dimension, whereas the trailing signal is vertical if it occurred during the second dimension electrophoresis proceeded. Detection of these perpendicular trailing signals serves to identify the supercoiled (CCC) form and its corresponding nicked (OC) form in N/N 2D gels (2,3,6,11,22,23). Two such signals were clearly detected in Figure 3A. They allowed us to identify the supercoiled form of non-replicating plasmids (CCC) and its corresponding nicked form (OC). They also allowed us to identify the most abundant supercoiled form of the partially replicated molecule (1.26× CCCRI) and

its corresponding nicked form (1.26× OCRI). Double-stranded breaks can also occur during DNA isolation, although less frequently. They convert circular plasmids into linear molecules of the same mass regardless of the site where breakage occurred. The spot detected below the OC signal in Figure 3A occurred on top of the linear arc and corresponded to linear forms of pBR18-TerE@StyI. This autoradiogram revealed that the population of partially replicated molecules occurred as a family of topoisomers in which strongly supercoiled topoisomers were highly abundant. The autoradiogram also showed that the vast majority of replicating plasmids had a fork stalled at TerE. In other words, it seemed that *in vivo* pBR18-TerE@StyI occurred in only two basic forms: the non-replicating CCC form (1.0×) and the partially replicated RI with a stalled fork containing an internal bubble (1.26× CCCRIs). Although most of the 1.26× CCCRIs showed a high level of negative supercoiling and high electrophoretic mobility, a few topoisomers showing slightly lower mobility were observed. A new DNA sample was prepared specifically enriched for the molecules responsible for the spot designated 1.26× OCRI (circled in the autoradiogram shown in Fig. 3A). These molecules were eluted from agarose gels and the DNA sample examined under an electron microscope. Figure 3C shows an electron

micrograph of one representative molecule, with a diagrammatic interpretation in Figure 3D. The vast majority of the molecules that were examined exhibited the same pattern. Repeated measurements indicated that the unreplicated arm represented 74% of the molecule. Correspondingly, the two identical replicated arms represented 26% of the plasmid. These numbers precisely matched the expected figures, as for this plasmid the mass of the accumulated RI was estimated to be 1.26 times the mass of non-replicating molecules (Fig. 1A).

Undigested pBR18-TerE@*EcoRI* DNA was also analyzed by N/N 2D agarose gel electrophoresis without ethidium bromide in the second dimension. An autoradiogram of this gel is shown in Figure 3E, together with a diagrammatic interpretation in Figure 3F. Once again, to confirm that the molecules responsible for the signal designated 1.57× OCRI in Figure 3E were indeed the nicked forms of partially replicated plasmids, we prepared a new DNA sample that was enriched for the molecules responsible for the spot designated 1.57× OCRI (circled in the autoradiogram shown in Fig. 3E). Figure 3G shows an electron micrograph of a representative molecule with a diagrammatic interpretation in Figure 3H. Once again, most of the molecules of this sample exhibited the same pattern. Repeated measurements indicated that in this case the unreplicated arm represented 43% of the plasmid. Correspondingly, the two identical replicated arms represented 57% of the plasmid. Once again, these numbers precisely matched the expected figures, as for pBR18-TerE@*EcoRI* the mass of the accumulated RI was estimated to be 1.57 times the mass of non-replicating molecules (Fig. 1C).

The most significant differences between the autoradiograms of these undigested samples shown in Figure 3A and E correspond to the number and position of CCCRI and OCRI, respectively. Whereas for pBR18-TerE@*StyI* most of the accumulated RIs showed the highest mobility observed, in the case of pBR18-TerE@*EcoRI* the electrophoretic mobility of CCCRI ranged between the most abundant (the one showing the highest mobility) and another showing almost the same mobility as the nicked forms (Fig. 3E). This observation confirms that the topology of RIs differs at different replication stages and suggests that plasmids become progressively relaxed as replication advances.

Chloroquine and ethidium bromide are planar molecules that can intercalate between the two strands of the DNA double helix. This intercalation causes a reduction in DNA twist. As *in vivo* bacterial plasmids are negatively supercoiled, the drugs remove negative supercoiling first and add net positive supercoiling only after all native negative supercoiling has been removed. We wanted to know whether the effects of these drugs were alike for non-replicating and partially replicated plasmids. To answer this question, four series of experiments were performed where pBR18-TerE@*StyI* and pBR18-TerE@*EcoRI* were analyzed in N/N 2D gels where the second dimension occurred without or in the presence of increasing concentrations of either chloroquine or ethidium bromide. The highest concentration chosen for each drug was the minimum required that induced at least some of the non-replicating DNA molecules to migrate with the same electrophoretic mobility as in the absence of the drugs. All the experiments were run under similar electrophoretic conditions except for the concentration of the intercalating agents in the second dimension. To make comparisons reliable, the different autoradiograms were

aligned in such a way that OC and OCRI, whose migration is not affected by the drugs, coincided exactly for all the autoradiograms within a series. Figure 4 shows the chloroquine series for pBR18-TerE@*StyI* (upper panels) and pBR18-TerE@*EcoRI* (lower panels). In both series the behavior of non-replicating forms (CCC) and partially replicated forms (CCCRI) were notably different. At low drug concentrations (0.5 and 10 µg/ml) CCC plasmids showed reduced mobility and at 10 µg/ml at least some of them migrated with the same mobility exhibited by the nicked (OC) forms in both cases. At higher concentrations (20–100 µg/ml) the CCC forms moved with increasingly higher mobility and at the highest concentration of the drug employed (100 µg/ml) a significant number of CCC plasmids migrated with the same mobility as in the absence of chloroquine. This observation indicated that at low drug concentrations, non-replicating CCC forms showed progressively lower levels of negative supercoiling until they were completely relaxed. Higher concentrations induced net positive supercoiling, which in turn led the plasmids to move with increasing mobility in the gel.

The behavior of partially replicated plasmids (CCCRI) was significantly different in both cases. As in the case of their non-replicating counterparts, at low concentrations of chloroquine (0.5 and 10 µg/ml) CCCRI showed progressively lower mobility and at 10 µg/ml at least some of them moved with the same mobility exhibited by the nicked (OCRI) forms. However, higher drug concentrations (20–100 µg/ml) did not change the mobility of CCCRI and at the highest concentration of chloroquine employed (100 µg/ml), which caused non-replicating (CCC) forms to attain the same mobility they showed in the absence of the drug, CCCRI still migrated with the same mobility exhibited by the nicked (OCRI) forms. This observation implied that in the presence of up to 100 µg/ml chloroquine partially replicated plasmids (CCCRI) were unable to sustain positive supercoiling.

We wanted to know whether non-replicating (CCC forms) and partially replicated plasmids (CCCRI) behaved in the same manner in the presence of increasing concentrations of another intercalator, such as ethidium bromide. Figure 5 shows the ethidium bromide series for pBR18-TerE@*StyI* (upper panels) and pBR18-TerE@*EcoRI* (lower panels). The results obtained were similar to those for the chloroquine series (Fig. 4), except for the 2D gels where the second dimension was run in the presence of the highest concentration of ethidium bromide employed (0.3 µg/ml). In these two singular cases the CCCRI did gain some mobility above the mobility exhibited by their nicked (OCRI) counterparts, and this difference was significantly more prominent in the case of pBR18-TerE@*StyI*. On average, induction of positive supercoiling by chloroquine and ethidium bromide was higher for pBR18-TerE@*StyI*. Another interesting observation that was particularly evident in the case of pBR18-TerE@*EcoRI* concerned the shape of the arc corresponding to CCCRI. Topoisomers with different ΔLk values showed different mobilities in the first dimension in the absence of the drug. When the second dimension occurred in the presence of ethidium bromide, however, CCCRI started to move with the same mobility as their OCRI counterparts as soon as they lost their native negative supercoiling. As this native negative supercoiling was still present throughout the first dimension of all the 2D gels in the series, its progressive elimination in the

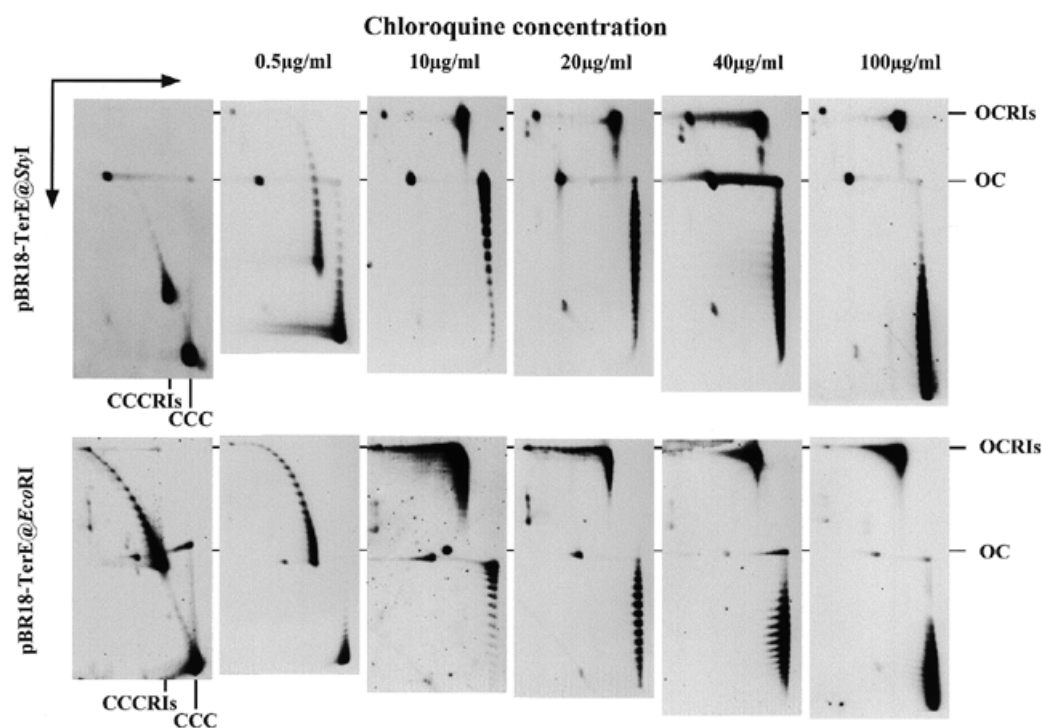


Figure 4. Autoradiograms of 2D gels corresponding to pBR18-TerE@*StyI* (upper) and pBR18-TerE@*EcoRI* (lower) where the second dimension occurred without (left) or in the presence of different concentrations of chloroquine (concentrations in µg/ml are indicated at the top). All the autoradiograms were aligned so that the positions of the OC and OCRIs, which are not affected by drug concentration, coincided. The positions of the CCC and CCCRIs are indicated only in the autoradiograms corresponding to untreated panels (left).

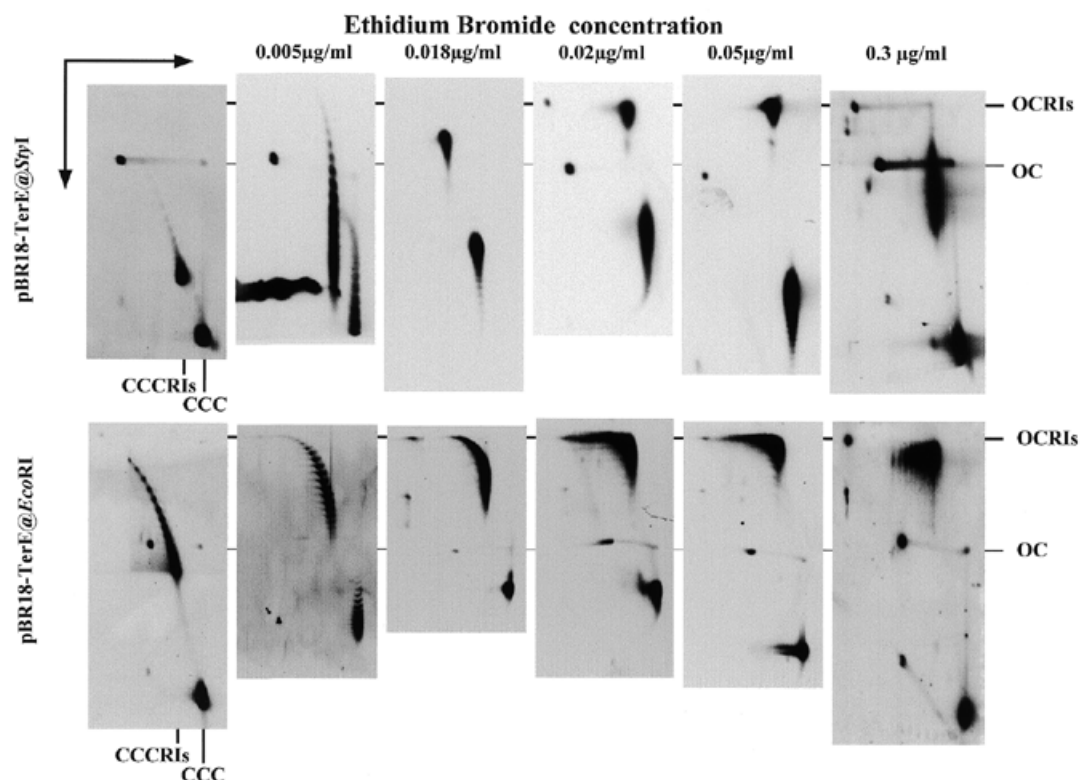


Figure 5. Autoradiograms of 2D gels corresponding to pBR18-TerE@*StyI* (upper) and pBR18-TerE@*EcoRI* (lower) where the second dimension occurred without (left) or in the presence of different concentrations of ethidium bromide (concentrations in µg/ml are indicated at the top). All the autoradiograms were aligned so that the positions of the OC and OCRIs, which are not affected by drug concentration, coincided. The positions of the CCC and CCCRIs are indicated only in the autoradiograms corresponding to untreated panels (left).

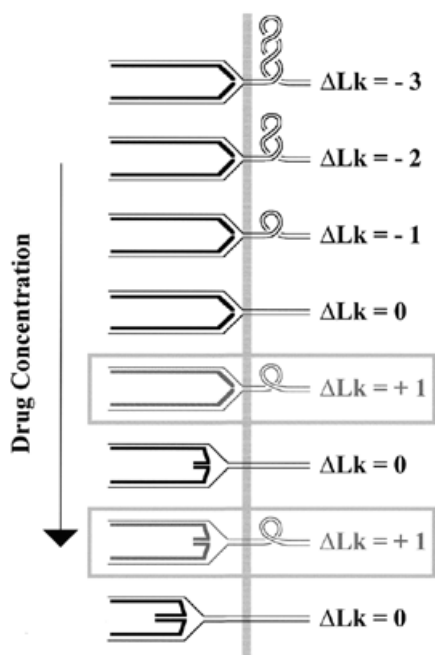


Figure 6. Diagrammatic model illustrating how the ΔLk value of a DNA segment containing a stalled fork might change as the concentration of chloroquine or ethidium bromide increases. At low concentrations of the drug the native negative supercoiling would progressively diminish until the molecule becomes completely relaxed ($\Delta Lk = 0$). From this point on, increasing concentrations of the drug would induce a net positive supercoiling. However, as soon as the ΔLk value becomes positive, nascent strands would separate from their corresponding parental strands and re-anneal with each other, leading to fork reversal. Each positive ΔLk eliminated would force fork reversal to advance 10 bp [adapted from Alexandrov *et al.* (31)].

second dimension in the presence of increasing concentrations of the drug led to a change in the angle of the arc corresponding to CCCRIs. This angle was smooth without ethidium bromide; it was slightly sharper at 0.005 $\mu\text{g/ml}$ and became notably abrupt with 0.02 $\mu\text{g/ml}$ and higher concentrations of the drug. Moreover, CCCRI topoisomers that exhibited different mobilities in the first dimension without ethidium bromide showed the same mobility in the second dimension even in the presence of 0.3 $\mu\text{g/ml}$, at which their electrophoretic mobility was slightly higher than the mobility of their OCRI counterparts.

The different behaviors of non-replicating CCC forms and CCCRIs in the presence of chloroquine and ethidium bromide could be due to replication fork reversal (10). This phenomenon would take place as soon as CCCRIs were forced to acquire net positive supercoiling (Fig. 6). Molecules containing reversed forks were readily observed under an electron microscope when linear DNA molecules containing an internal bubble were extracted from low melting point agarose gels after heating and β -agarase digestion (14). For RIs containing an internal bubble, progression of fork reversal is characterized by the presence of an additional fourth arm and a concomitant reduction in the size of the bubble (14). To test whether fork reversal was indeed responsible for the peculiar effects of chloroquine and ethidium bromide on the electrophoretic mobility of CCCRIs that were observed in Figures 4 and 5, new DNA samples were prepared that were enriched for

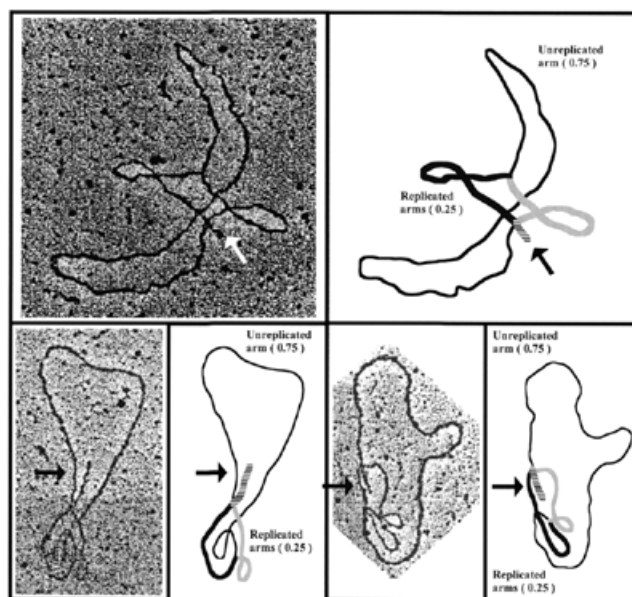


Figure 7. Electron micrographs of intact forms of pBR18-TerE@StyI showing reversed forks. CCCRIs were eluted from agarose gels in the presence of 100 $\mu\text{g/ml}$ chloroquine, following which the drug was removed by washing thoroughly with distilled water and the CCCRIs treated with topoisomerase I to eliminate all negative supercoiling, exposed to 100 $\mu\text{g/ml}$ chloroquine again and examined under an electron microscope. Black lines represent unreplicated DNA, stippled lines replicated arms and horizontally striped lines the newly formed nascent-nascent fourth arm that resulted from fork reversal (indicated by arrows). Numbers denote the percentage contour length of unreplicated and replicated arms.

CCCRIs eluted from 2D gels similar to those shown in Figures 4 and 5 where the second dimension occurred with 100 $\mu\text{g/ml}$ chloroquine or 0.3 $\mu\text{g/ml}$ ethidium bromide. These DNA samples were examined under an electron microscope looking for CCCRIs containing reversed forks. No such molecules were detected (data not shown). The interpretation of these results will be discussed later.

To induce plasmids to acquire net positive supercoiling, intercalating drugs first had to remove all native negative supercoiling. This situation might have hampered the effects of both drugs. On the other hand, the results obtained so far indicate that not all positive supercoiling was eliminated in the presence of 0.3 $\mu\text{g/ml}$ ethidium bromide. Besides, we showed earlier that the sensitivity to both drugs was higher for pBR18-TerE@StyI. To increase the induction of net positive supercoiling we prepared a new DNA sample that was enriched for the CCCRIs of pBR18-TerE@StyI where all the native negative supercoiling had been removed by topoisomerase I before exposure to 100 $\mu\text{g/ml}$ chloroquine. In this way, chloroquine would induce net positive supercoiling with no need to first remove native negative supercoiling (24). After addition of 100 $\mu\text{g/ml}$ chloroquine this DNA sample was examined under an electron microscope. Representative molecules corresponding to this sample are shown in Figure 7. Even though not all the molecules exhibited fork reversal, the phenomenon was evident in several cases. It should be noted that in order to eliminate false positives, unreplicated and replicated arms were carefully measured. For a plasmid to be

accepted as a genuine molecule showing fork reversal, the unreplicated arm had to account for $\geq 74\%$ of the plasmid. Both replicated arms should measure alike and must account for $\leq 26\%$ of the plasmid. Finally, the fourth arm should account for the difference in size between the unreplicated and replicated arms observed between the problem form and the corresponding nicked form (Fig. 1B and D). The examples depicted in Figure 7 comply with all these restrictions. Most of the molecules with reversed forks showed a Holliday-like junction at only one fork, but some molecules were observed with Holliday-like junctions at both forks (data not shown). In those cases with a single Holliday-like junction, however, we could not determine whether it occurred at the origin or the stalled fork. Curiously, in the case of pBR18-TerE@*StyI* analyzed in the presence of 0.3 $\mu\text{g/ml}$ ethidium bromide, detection of a discrete spot to the left of the unreplicated CCC forms strongly suggests that in a few cases fork reversal proceeded until the re-annealed nascent strands were completely extruded. This was observed neither for pBR18-TerE@*EcoRI* nor for any plasmid analyzed in the presence of 100 g/ml chloroquine (Figs 4 and 5).

In summary, the observation that partially replicated plasmids do not sustain positive supercoiling is likely due to fork reversal. But in order to reveal Holliday-like junctions under the electron microscope, very high levels of positive supercoiling have to be induced.

DISCUSSION

TerE is one of various polar replication terminators of the *E. coli* chromosome (8,9). Replication forks stop as soon as they meet a Ter-TUS complex in the proper orientation due to the anti-helicase activity of this complex (25). *Escherichia coli* DH5 α F' cells express TUS constitutively. If all plasmid molecules in a cell bind TUS, none would complete replication and cells would not be able to grow under selection. How did pBR18-TerE@*StyI* and pBR18-TerE@*EcoRI* manage to complete replication in these cells? The equilibrium dissociation constant of TUS varies for different Ter sites, TerB being the most efficient and TerE one of the weakest (18). Indeed, the doubling time for cells transformed with a plasmid carrying TerB was significantly longer than the doubling time for cells transformed with pBR18-TerE@*StyI* or pBR18-TerE@*EcoRI*, which in turn was much longer than the doubling time for cells transformed with pBR18 carrying no Ter site (data not shown). We believe that DH5 α F' cells transformed with pBR18-TerE@*StyI* or pBR18-TerE@*EcoRI* were able to grow in the presence of ampicillin because not all plasmid molecules in a cell bound TUS. Those few plasmids that did not bind TUS were able to complete replication unimpaired and allowed the cells to grow under selection. Changes in the replication termination system are known to affect plasmid copy number (26,27). We propose that in these cells plasmid copy number would be a function of the equilibrium dissociation constant of TUS for the Ter site present in the plasmid. As plasmid copy number lessens; the cell doubling time would lengthen.

Knotted bubbles

In those plasmids containing two inversely oriented ColE1 origins, the replication fork initiated at one origin halts as it reaches the silent origin. This leads to the accumulation of partially replicated RIs where knots form within the replicated

portion of the plasmid (12). Most of the nodes of these knotted bubbles have a positive sign (21), indicating that they resulted from *in vivo* action of type II topoisomerases on negatively twisted precatenanes (28). These knotted RIs are detected only when the ΔLk of the plasmid is eliminated, either by nicking or digestion with a restriction enzyme that cuts outside the bubble. The autoradiograms shown in Figure 2A and C demonstrate that these knotted bubbles also form when the replication fork is blocked at the TerE-TUS complex. The observation that there were many more and complex knotted bubbles in pBR18-TerE@*EcoRI* indicates that the number of negatively twisted precatenanes increases as replication progresses, at least during the first half of the replication process. Since supercoiling can diffuse across the replication fork (29,30), the distribution of supercoils and precatenanes is expected to change as replication progresses. At the beginning the replicated region would be too small to accommodate a large number of precatenanes, but as it becomes larger the number of precatenanes is also expected to increase. However, topoisomerase IV removes precatenanes and therefore their number should decrease as the completion of replication approaches (30–32). Further experiments are needed to demonstrate whether or not the number of knotted bubbles also decreases at the end of replication.

Electrophoretic mobility of CCCRIs

Progression of the replication fork generates positive supercoiling ahead of the fork due to unwinding of the parental strands by DNA helicase. In bacteria this positive stress is released by DNA gyrase acting ahead of the fork and topoisomerase IV removing precatenanes in the replicated region (30–32). The observation that for pBR18-TerE@*EcoRI* CCCRIs were observed exhibiting lower ΔLk values (Fig. 3A and E) suggests that CCCRIs become progressively relaxed as replication advances. These results, however, should be examined with caution, as they do not necessarily reflect the situation during unimpaired DNA replication *in vivo*. In those plasmids containing stalled forks where replication stopped due to the anti-helicase activity of the TerE-TUS complex (9) there might be an excess of negative stress due to the continuous action of DNA gyrase. Furthermore, the observation that a significant number of partially replicated RIs contained knotted bubbles (Fig. 2) and that these knotted RIs were not detected unless all ΔLk was eliminated indicates that the signals detected in the autoradiograms shown in Figure 3A and E do not represent all the CCCRIs of the population, as a selected sub-population of supercoiled RIs (formed by plasmids containing knotted bubbles) remained undetected. Despite all these remarks, however, the differences observed between pBR18-TerE@*StyI* and pBR18-TerE@*EcoRI* strongly suggest that the topology of CCCRIs changes dramatically as plasmid replication advances (30–32).

Positive supercoiling and replication fork reversal

The autoradiograms shown in Figures 4 and 5 allowed us to study, in the same gel, how non-replicated and partially replicated plasmids reacted to chloroquine or ethidium bromide *in vitro*. Comparison of the results obtained using different plasmids and different concentrations of both drugs helped us to foresee the dynamics of these changes as replication advanced.

For non-replicating molecules the results confirmed the original observations of Bauer and Vinograd (33). Increasing the concentration of chloroquine or ethidium bromide leads to a gradual decrease in the writhe of the molecules until they become completely relaxed. When more drug was added the DNA began to supercoil in the opposite direction.

The behavior of partially replicated plasmids was completely different. At low drug concentrations both CCC and CCCRI were progressively relaxed, but when more drugs were added CCCRI did not supercoil in the opposite direction. In other words, in partially replicated molecules chloroquine and ethidium bromide were able to remove negative supercoiling but were unable to introduce net positive supercoiling. An important exception should be noted for the higher concentration of ethidium bromide employed, 0.3 $\mu\text{g/ml}$ (Fig. 5). This was the single case where for both plasmids the electrophoretic mobility of CCCRI did increase, although the rise was notably lower than that exhibited by their non-replicating counterparts in the same gels. Also, this ethidium bromide-induced rise in the electrophoretic mobility of CCCRI was significantly higher for pBR18-TerE@*StyI*. In both cases, however, the signal had an oblong shape and no discrete horizontal bands could be discerned.

Regression of replication forks with concomitant formation of Holliday-like junction structures was originally proposed several years ago as a necessary step in a model for replication repair in mammalian cells (34). It was claimed that this phenomenon could take place specifically at arrested replication forks (35,36) and molecules containing reversed forks were actually visualized under the electron microscope in digested plasmids containing stalled forks (14). More recently it was proposed that the positive torsional strain induced by high concentrations of ethidium bromide leads to the formation of these structures at replication forks (10). It is important to note that in a partially replicated molecule regression of a replication fork implies shrinkage of the previously formed bubble and the appearance of a fourth arm, the length of which should be proportional to the bubble shrinkage (Fig. 5). Postow and co-workers (10) carefully examined the thermodynamics of fork reversal. They claim that formation of these structures would require very little energy (5 kcal/mol, compared to the 20–28 kcal/mol needed for cruciform extrusion). Once formed, however, there would be no difference between progression of fork reversal and branch migration. Hence, progression of fork reversal would also reduce superhelical stress in such a way that one positive supercoil would be lost for each 10 bp fork reversal advance (37). We believe that these figures explain the behavior of the CCCRI we observed for pBR18-TerE@*StyI* and pBR18-TerE@*EcoRI* in the presence of different concentrations of chloroquine and ethidium bromide. In all the N/N 2D gels shown in Figures 4 and 5 the effect of one ΔLk on electrophoretic mobility was considerable. However, formation of a reversed fork and advancement of fork reversal would have very little if any effect on electrophoretic mobility. For this reason CCCRI containing reversed forks are expected to show the same electrophoretic mobility as their nicked counterparts (OCRIs). For both drugs induction of positive supercoiling was more efficient in pBR18-TerE@*StyI*. In this plasmid the unreplicated portion (the only relevant target for chloroquine or ethidium bromide induction of positive supercoiling) accounted for 74% of the plasmid length, whereas this figure

was reduced to 43% in the case of pBR18-TerE@*EcoRI*. This higher sensitivity of pBR18-TerE@*StyI* explains why the effect of the drugs adding positive supercoiling was more efficient for this plasmid as compared to pBR18-TerE@*EcoRI*. It also explains why the regain of electrophoretic mobility detected for CCCRI in the presence of 0.3 $\mu\text{g/ml}$ ethidium bromide was significantly higher for this plasmid as compared to pBR18-TerE@*EcoRI*. Together, these observations also explain why fork reversal was finally detected under the electron microscope in some molecules of pBR18-TerE@*StyI* when all negative supercoiling had been eliminated by topoisomerase I prior to induction of positive supercoiling with 100 $\mu\text{g/ml}$ chloroquine (Fig. 7).

In summary, we confirmed that in partially replicated plasmids positive supercoiling can lead to replication fork reversal (10). This explains why CCCRI did not regain electrophoretic mobility after all negative supercoiling had been removed. There are significant differences, however, between the observations by Postow and co-workers (10) and us. First, they used chloroquine 2D gels and a significantly low concentration of chloroquine (10–11 $\mu\text{g/ml}$) to show that CCCRI do not regain electrophoretic mobility after all negative supercoiling has been removed and a very high concentration of ethidium bromide (12.6 $\mu\text{g/ml}$) to show fork reversal by restriction enzyme digestion and atomic force microscopy. We used Brewer–Fangman N/N 2D gels (2,6) and electron microscopy to show the effects of different concentrations of chloroquine (0.5–100 $\mu\text{g/ml}$) and ethidium bromide (0.005–0.3 $\mu\text{g/ml}$) on CCCRI as well as on non-replicating plasmids (CCC). Using atomic force microscopy Postow and co-workers (10) showed that partially replicated plasmids with reversed forks were supercoiled when treated with 12.6 $\mu\text{g/ml}$ ethidium bromide. The authors claimed that acquisition of ΔLk by these plasmids was an artifact caused during the deposition procedure for atomic force microscopy. However, we found that CCCRI did gain electrophoretic mobility even when exposed to 25 times less ethidium bromide (Fig. 5). Why is not all positive supercoiling absorbed by fork reversal? It could be that the energy required increases as fork reversal advances. Another possibility is that intercalation of more and more ethidium bromide somehow prevents denaturation of the parental–nascent duplexes. As a consequence, advancement of fork reversal would stop and positive supercoiling would start to build up. Further experiments are required to elucidate this point. Finally, another difference between our results and those obtained by Postow and co-workers (10) is that we found fork reversal to occur predominantly at only one fork per molecule, whereas they claim it occurs at one or both forks with approximately the same frequency. Figure 8 shows a diagram of a ColE1 bubble with a stalled fork. After RNA removal, the lengths of the leading and lagging strands differ at both ends of the accumulated bubble, the replication origin and the fork arrest site. At the origin the lagging nascent strand extends 17 bp beyond the point where the leading strand begins (13,38). At the fork arrest site, on the other hand, the leading nascent strand ends 3 bp before the TUS-binding site, whereas the lagging strand stops way back, 63–65 bp before (13,39). Due to these differences in the length of nascent strands at the origin and the fork arrest site, their re-annealing during fork reversal is expected to be favored at the origin.

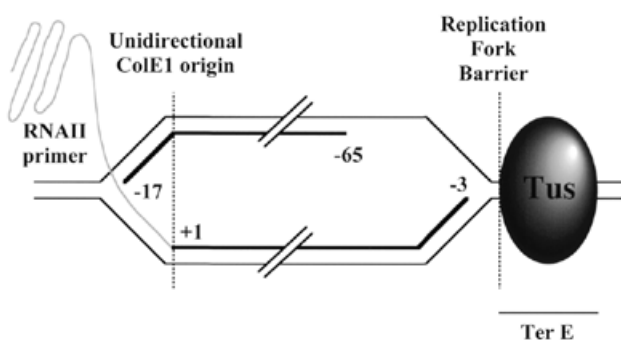


Figure 8. Diagram of the structure of a replication bubble where initiation occurred at the ColE1 origin and the replication fork stopped at the Ter-TUS complex. Thin lines represent parental DNA while thick lines represent nascent DNA. The two vertical dashed lines mark the position of the origin and the proximal end of the TUS recognition sequence, respectively. Numbers indicate base pairs before (-) and after (+) the origin and the right end of the TUS recognition sequence.

In vivo implications

In the last couple of years several authors have reviewed the relationship between stalled replication forks and genetic recombination (40–43). All of them have emphasized that DNA resolvases that specifically recognize Holliday junctions are driven to stalled forks *in vivo* (35,36). The mechanisms leading to the formation of Holliday junctions at stalled forks were investigated *in vitro* as well as *in vivo* (44–47). The results obtained in the present study together with those published by others (10) show that positive supercoiling can also lead to replication fork reversal with concomitant formation of a fourth arm, at least *in vitro*. This structure would be indistinguishable from a genuine Holliday junction. We believe that *in vivo* the DNA in the vicinity of a stalled fork could be positively supercoiled, at least transiently, if DNA helicase action is faster than topoisomerases can relax the stress (48). This structure would be recognized by DNA resolvases to start DNA recombination. It is important to note though that although high levels of positive supercoiling are required to detect fork reversal by restriction enzyme digestion or electron microscopy, significantly less positive ΔLk is needed to generate the formation of Holliday-like junctions at arrested forks, as shown by the fact that CCCRs did not regain electrophoretic mobility immediately after all negative supercoiling had been removed (Figs 4 and 5). These observations *in vitro* suggest that low levels of positive supercoiling in the vicinity of an arrested fork would be enough to trigger the formation of Holliday-like junctions *in vivo*.

ACKNOWLEDGEMENTS

We are grateful to Alicia Sánchez Gorostiaga for help and support throughout the course of this study and to Pilar Robles for technical assistance. This work was partially supported by grants PM97-0138 and PGC PB98-048 from the Spanish Comisión Interministerial de Ciencia y Tecnología (CICYT), 99/0850 from the Spanish Fondo de Investigación Sanitaria (FIS), 08.6/0016/1997 from the Comunidad Autónoma de Madrid (CAM) and from the Swiss National Science Foundation to J.M.S. (31-63418) and A.S. (31-61636 and 31-58841).

REFERENCES

- Bell, L. and Byers, B. (1983) Separation of branched from linear DNA by two-dimensional gel electrophoresis. *Anal. Biochem.*, **130**, 527–535.
- Friedman, K.L. and Brewer, B.J. (1995) Analysis of replication intermediates by two-dimensional agarose gel electrophoresis. In Campbell, J.L. (ed.), *DNA Replication*. Academic Press, San Diego, CA, Vol. 262, pp. 613–627.
- Martín-Parras, L., Lucas, I., Martínez-Robles, M.L., Hernández, P., Krimer, D.B., Hyrien, O. and Schwartzman, J.B. (1998) Topological complexity of different populations of pBR322 as visualized by two-dimensional agarose gel electrophoresis. *Nucleic Acids Res.*, **26**, 3424–3432.
- Sundin, O. and Varshavsky, A. (1980) Terminal stages of SV40 DNA replication proceed via multiply intertwined catenated dimers. *Cell*, **21**, 103–114.
- Sundin, O. and Varshavsky, A. (1981) Arrest of segregation leads to accumulation of highly intertwined catenated dimers: dissection of the final stages of SV40 DNA replication. *Cell*, **25**, 659–669.
- Brewer, B.J. and Fangman, W.L. (1987) The localization of replication origins on ARS plasmids in *S. cerevisiae*. *Cell*, **51**, 463–471.
- Brewer, B.J., Sena, E.P. and Fangman, W.L. (1988) Analysis of replication intermediates by two-dimensional agarose gel electrophoresis. *Cancer Cells*, **6**, 229–234.
- Hill, T.M., Pelletier, A.J., Tecklenburg, M.L. and Kuempel, P.L. (1988) Identification of the DNA sequence from *E. coli* terminus region that halts replication forks. *Cell*, **55**, 459–466.
- Bastia, D. and Mohanty, B.K. (1996) Mechanisms for completing DNA replication. In DePamphilis, M.L. (ed.), *DNA Replication in Eukaryotic Cells*. Cold Spring Harbor Laboratory Press, Cold Spring Harbor, NY, pp. 177–215.
- Postow, L., Ullsperger, C., Keller, R.W., Bustamante, C., Vologodskii, A.V. and Cozzarelli, N.R. (2001) Positive torsional strain causes the formation of a four-way junction at replication forks. *J. Biol. Chem.*, **276**, 2790–2796.
- Martín-Parras, L., Hernández, P., Martínez-Robles, M.L. and Schwartzman, J.B. (1992) Initiation of DNA replication in ColE1 plasmids containing multiple potential origins of replication. *J. Biol. Chem.*, **267**, 22496–22505.
- Viguera, E., Hernández, P., Krimer, D.B., Boistov, A.S., Lurz, R., Alonso, J.C. and Schwartzman, J.B. (1996) The ColE1 unidirectional origin acts as a polar replication fork pausing site. *J. Biol. Chem.*, **271**, 22414–22421.
- Santamaría, D., Hernández, P., Martínez-Robles, M.L., Krimer, D.B. and Schwartzman, J.B. (2000) Premature termination of DNA replication in plasmids carrying two inversely oriented ColE1 origins. *J. Mol. Biol.*, **300**, 75–82.
- Viguera, E., Hernández, P., Krimer, D.B., Lurz, R. and Schwartzman, J.B. (2000) Visualisation of plasmid replication intermediates containing reversed forks. *Nucleic Acids Res.*, **28**, 498–503.
- Sogo, J.M., Stasiak, A., De Bernardin, W., Losa, R. and Koller, T. (1987) Binding of proteins to nucleic acids. In Somerville, J. and Scheer, U. (eds), *Electron Microscopy in Molecular Biology. A Practical Approach*. IRL Press, Oxford, UK, pp. 61–79.
- Shishido, K., Komiyama, M. and Ikawa, S. (1987) Increased production of a knotted form of plasmid pBR322 DNA in *Escherichia coli* DNA topoisomerase mutants. *J. Mol. Biol.*, **195**, 215–218.
- Shishido, K., Ishii, S. and Komiyama, N. (1989) The presence of the region on pBR322 that encodes resistance to tetracycline is responsible for high levels of plasmid DNA knotting in *Escherichia coli* DNA topoisomerase I deletion mutant. *Nucleic Acids Res.*, **17**, 9749–9759.
- Gottlieb, P.A., Wu, S., Zhang, X., Tecklenburg, M., Kuempel, P. and Hill, T.M. (1992) Equilibrium, kinetic and footprinting studies of the Tus-Ter protein-DNA interaction. *J. Biol. Chem.*, **267**, 7434–7443.
- Viguera, E., Rodríguez, A., Hernández, P., Krimer, D.B., Trellez, O. and Schwartzman, J.B. (1998) A computer model for the analysis of DNA replication intermediates by two-dimensional agarose gel electrophoresis. *Gene*, **217**, 41–49.
- Santamaría, D., de la Cueva, G., Martínez-Robles, M.L., Krimer, D.B., Hernández, P. and Schwartzman, J.B. (1998) DnaB helicase is unable to dissociate RNA-DNA hybrids—its implication in the polar pausing of replication forks at ColE1 origins. *J. Biol. Chem.*, **273**, 33386–33396.
- Sogo, J.M., Stasiak, A., Martínez-Robles, M.L., Krimer, D.B., Hernández, P. and Schwartzman, J.B. (1999) Formation of knots in partially replicated DNA molecules. *J. Mol. Biol.*, **286**, 637–643.

22. Schwartzman, J.B., Adolph, S., Martín-Parras, L. and Schildkraut, C.L. (1990) Evidence that replication initiates at only some of the potential origins in each oligomeric form of Bovine Papillomavirus Type 1 DNA. *Mol. Cell. Biol.*, **10**, 3078–3086.
23. Martín-Parras, L., Hernández, P., Martínez-Robles, M.L. and Schwartzman, J.B. (1991) Unidirectional replication as visualized by two-dimensional agarose gel electrophoresis. *J. Mol. Biol.*, **220**, 843–853.
24. Torheim, N.K. and Skarstad, K. (1999) *Escherichia coli* SeqA protein affects DNA topology and inhibits open complex formation at oriC. *EMBO J.*, **18**, 4882–4888.
25. Khatri, G.S., MacAllister, T., Sista, P.R. and Bastia, D. (1989) The replication terminator protein of *E. coli* is a sequence-specific contra-helicase. *Cell*, **59**, 667–674.
26. Krabbe, M., Zabielski, J., Bernander, R. and Nordstrom, K. (1997) Inactivation of the replication-termination system affects the replication mode and causes unstable maintenance of plasmid R1. *Mol. Microbiol.*, **24**, 723–735.
27. Paulsson, J. and Ehrenberg, M. (1998) Trade-off between segregational stability and metabolic burden: a mathematical model of plasmid ColE1 replication control. *J. Mol. Biol.*, **279**, 73–88.
28. Postow, L., Peter, B.J. and Cozzarelli, N.B. (1999) Knot what we thought before: the twisted story of replication. *Bioessays*, **21**, 805–808.
29. Champoux, J.J. and Been, M.D. (1980) Topoisomerases and the swivel problem. In Alberts, B. (ed.), *Mechanistic Studies of DNA Replication and Genetic Recombination*. Academic Press, New York, NY, pp. 809–815.
30. Peter, B.J., Ullsperger, C., Hiasa, H., Marians, K.J. and Cozzarelli, N.R. (1998) The structure of supercoiled intermediates in DNA replication. *Cell*, **94**, 819–827.
31. Alexandrov, A.I., Cozzarelli, N.R., Holmes, V.F., Khodursky, A.B., Peter, B.J., Postow, L., Rybenkov, V. and Vologodskii, A.V. (1999) Mechanisms of separation of the complementary strands of DNA during replication. *Genetica*, **106**, 131–140.
32. Ullsperger, C., Vologodskii, A.A. and Cozzarelli, N.R. (1995) Unlinking of DNA by topoisomerases during DNA replication. In Lilley, D.M.J. and Eckstein, F. (eds), *Nucleic Acids and Molecular Biology*. Springer-Verlag, Berlin, Germany, pp. 115–142.
33. Bauer, W. and Vinograd, J. (1968) The interaction of closed circular DNA with intercalative dyes. *J. Mol. Biol.*, **33**, 141–171.
34. Higgins, N.P., Kato, K. and Strauss, B. (1976) A model for replication repair in mammalian cells. *J. Mol. Biol.*, **101**, 417–425.
35. Seigneur, M., Bidnenko, V., Ehrlich, S.D. and Michel, B. (1998) RuvAB acts at arrested replication forks. *Cell*, **95**, 419–430.
36. West, S.C. (1997) Processing of recombination intermediates by the RuvABC proteins. *Annu. Rev. Genet.*, **31**, 213–244.
37. Holloman, W.K., Wiegand, R., Hoessli, C. and Radding, C.M. (1976) Uptake of homologous single-stranded fragments by superhelical DNA: a possible mechanism for initiation of genetic recombination. *Proc. Natl Acad. Sci. USA*, **72**, 2394–2398.
38. Dasgupta, S., Masukata, H. and Tomizawa, J. (1987) Multiple mechanisms for initiation of ColE1 DNA replication DNA synthesis in the presence and absence of ribonuclease H. *Cell*, **51**, 1113–1122.
39. Mohanty, B.K., Sahoo, T. and Bastia, D. (1998) Mechanistic studies on the impact of transcription on sequence-specific termination of DNA replication and vice versa. *J. Biol. Chem.*, **273**, 3051–3059.
40. Cox, M.M., Goodman, M.F., Kreuzer, K.N., Sherratt, D.J., Sandler, S.J. and Marians, K.J. (2000) The importance of repairing stalled replication forks. *Nature*, **404**, 37–41.
41. Hyrien, O. (2000) Mechanisms and consequences of replication fork arrest. *Biochimie*, **82**, 5–17.
42. Marians, K.J. (2000) Replication and recombination intersect. *Curr. Opin. Genet. Dev.*, **10**, 151–156.
43. Michel, B. (2000) Replication fork arrest and DNA recombination. *Trends Biochem. Sci.*, **25**, 173–178.
44. McGlynn, P. and Lloyd, R.G. (2000) Modulation of RNA polymerase by (P)ppGpp reveals a RecG-dependent mechanism for replication fork progression. *Cell*, **101**, 35–45.
45. Seigneur, M., Ehrlich, S.D. and Michel, B. (2000) RuvABC-dependent double-strand breaks in dnaBts mutants require RecA. *Mol. Microbiol.*, **38**, 565–574.
46. McGlynn, P., Lloyd, R.G. and Marians, K.J. (2001) Formation of Holliday junctions by regression of nascent DNA in intermediates containing stalled replication forks: RecG stimulates regression even when the DNA is negatively supercoiled. *Proc. Natl Acad. Sci. USA*, **98**, 8235–8240.
47. Robu, M.E., Inman, R.B. and Cox, M.M. (2001) RecA protein promotes the regression of stalled replication forks *in vitro*. *Proc. Natl Acad. Sci. USA*, **98**, 8211–8218.
48. Bucka, A. and Stasiak, A. (2001) Replication forks under torsional strain. *Chemtracts Biochem. Mol. Biol.*, **14**, 166–173.